Non-Cartesian Parallel Imaging Reconstruction Using PRUNO-GROG

J. Zhang[1], and A. Shankaranarayanan[2]
[1]Global Applied Science Lab, GE HealthCare, Bethesda, MD, United States, [2]Global Applied Science Lab, GE HealthCare, Menlo Park, CA, United States

INTRODUCTION Pseudo-Cartesian GRAPPA in conjunction with GROG (PCG-GROG) [1] is an effective algorithm to reconstruct non-Cartesian parallel imaging data. Its reconstruction procedure can be simply divided into two sequential steps: gridding the undersampled non-Cartesian k-space samples onto the nearest Cartesian grids using GROG [2], and performing a pseudo GRAPPA data fitting based on the interpolated samples. However, the pseudo GRAPPA reconstruction is usually a cumbersome task as different fitting patterns need to be determined point by point. PRUNO [3, 4] is a generalized auto-calibrated reconstruction algorithm which uses local nulling kernels to find the optimal global fitting solution iteratively. During the reconstruction, PRUNO kernels are applied to all k-space locations, independent of the acceleration factor and undersampling patterns. We can thus replace the PCG step in [1] with PRUNO to bring out a more convenient and accurate algorithm. PRUNO-GROG is presented in this work, in which streamlined data calibration and reconstruction can be easily performed on the GROGed data, regardless of sampling trajectories. Promising preliminary results are shown on both phantom and *in vivo* images.

METHODS Fig 1 shows a comparison between PCG and PRUNO kernel applications following the GROG interpolation. For GRAPPA, as each missing sample needs to be directly synthesized from nearby available samples, both data calibration and reconstruction should strictly follow an appropriate template pattern. As GROG produces Cartesian samples from the non-Cartesian readout trajectories, multiple patterns are usually required, depending on the GRAPPA kernel size, as shown by the two blue boxes in the middle. In PRUNO, on the other hand, nulling kernels are purely small convolution windows that are independent of sampling patterns. To formulate the entire reconstruction into a linear system problem, these kernels are continuously applied to all k-space locations so that local sample correlations propagate and all k-space samples are eventually coupled together by the system nulling matrix [3] as $\mathbf{Nd} = \mathbf{0}$, where $\mathbf{d}$ is the vector of concatenated k-space data from all coils. The least mean square solution of missing samples ($\mathbf{d}_m$) are then synthesized from all acquired samples ($\mathbf{d}_a$) by solving this equation with an iterative CG algorithm.

The PRUNO-GROG reconstruction algorithm has been applied to both simulation and *in vivo* data. Matrix size of 256x256 and 8 channel coils were used in these experiments. Two types of trajectories were evaluated: interleaved variable-density spirals (VDS) and radial projections (RAD). Our full spiral sampling contains 24 interleaves and radial readout has 400 projections. Fully sampled k-space date were simulated or acquired first in each experiment and then undersampled according to the given reduction factor in each trial. The simulated multi-channel data were generated using pre-measured coil-sensitivity profiles. Normal complex noises were added, with [σ_N] corresponding to 0.2% of the maximum DC signal.

The *in vivo* scan was performed on a health volunteer by using a GRE sequence on a GE 1.5T scanner. A separate calibration scan was also performed to acquire 7 Cartesian lines as auto-calibration signal (ACS), which was used by both GROG and PRUNO data calibration. GROG calibration and interpolation was implemented using the method described in [1]. In PRUNO, 50 out of 200 (5x5x8) VDS nulling kernels were selected [4]. In each case, the output of GROG interpolation was directly applied as the initial guess of CG without further interpolation. Details of PRUNO reconstruction procedure can be found in [3, 4].

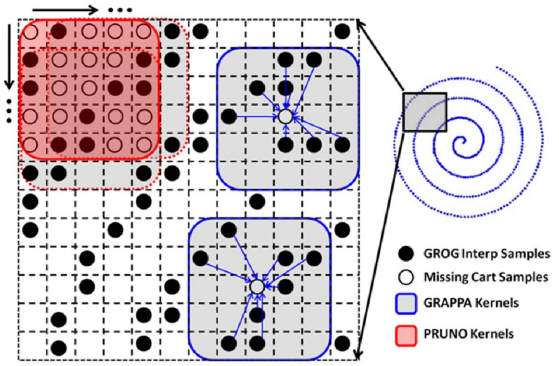

Figure 1: Kernel applications of PCG and PRUNO following the GROG interpolation of a spiral trajectory. Both PRUNO and GRAPPA kernels are 5x5 here. Multiple patterns of GRAPPA kernels are required to fit different missing samples (blue boxes). PRUNO kernels are independent of local sampling patterns and applied onto all k-space locations (red boxes).

RESULTS Given the same reduction factor, the system condition of PRUNO-GROG reconstruction in our experiment is much better than that of 1D Cartesian PRUNO, as both VDS and RAD may provide sampling acceleration in both directions. The CG algorithm thus converges much faster, taking only 10 to 20 iterations to stop. Fig 2 shows the reconstruction results of phantom at reduction factors of 2, 4, and 6 respectively. Each image is also compared with the original reference and the magnitude difference is shown below. Even at R=6, PRUNO-GROG yields good performance on the noisy data without producing noticeable aliasing artifacts. Fig 3 shows the reconstructed *in vivo* images at 2 and 4-fold. Fully-sampled GROG reconstruction [2] was provided as the reference for each trajectory. Despite of the SNR drop-off, all PRUNO-GROG images are in very good quality compared to the reference images.

DISCUSSION AND CONCLUSION Here we have demonstrated a new non-Cartesian parallel imaging method, termed PRUNO-GROG. Compared with PCG, PRUNO is much easier to be streamlined into the reconstruction flow and more accurate reconstruction is usually expected since PRUNO essentially finds the optimal missing sample solutions through linear fitting from all available data. The CG reconstruction offers good convergence speed for common 2D accelerated trajectories. However, the performance of PRUNO also depends on the accuracy of GROG operation, as the interpolation errors will propagate into the following CG iterations of PRUNO. Our preliminary results show that PRUNO-GROG has great potential as a feasible and reliable non-Cartesian parallel imaging algorithm.

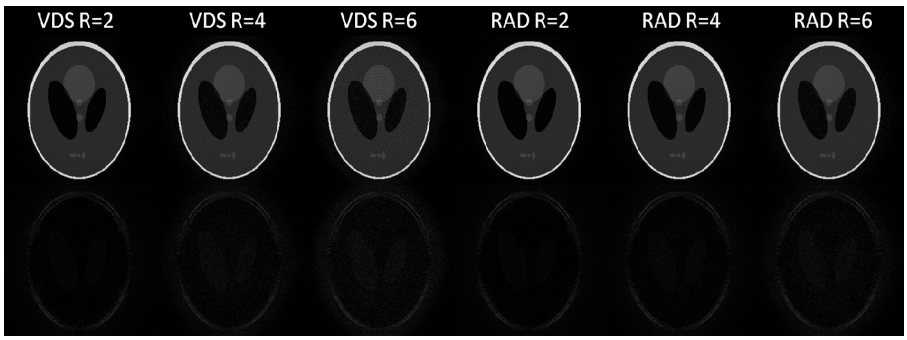

Figure 2: Phantom results. Top: reconstruction of PRUNO-GROG. Bottom: difference to the reference.

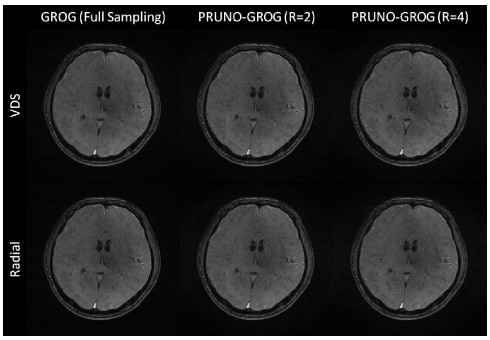

Figure 3: In vivo results.

REFERENCES

1. Seiberlich N, et al., Magn Recon Med, 59, 1127-1137, 2009; 2. Seiberlich N, et al., Magn Reson Med, 58, 1257-1265, 2007; 3. Zhang J, et al., Proc 16th ISMRM, #9, 2008; 4. Zhang J, et al, Proc 18th ISMRM #4907, 2010.